OPEN ACCESS

2nd International Electronic Conference on Entropy and Its Applications
15-30 November 2015

www.sciforum.net/conference/ecea-2

*Conference Proceedings Paper – Entropy*

# Exergy Analysis of a Syngas-Fueled Combined Cycle with Chemical-Looping Combustion and $CO_2$ sequestration

**Álvaro Urdiales[1], Ángel Jiménez[1,*], Javier Rodríguez[1] and Rafael Nieto[1]**

[1] Department of Energy Engineering, ETSII, Technical University of Madrid.
José Gutiérrez Abascal, 2, 28006, Madrid, Spain

* Author to whom correspondence should be addressed;
e-mail: a.jimenez@upm.es, tel.: +34 91 336 4262, fax: +34 91 336 4263

*Published: 5 November 2015*

---

**Abstract:** Fossil fuels are still needed extensively for power generation. Nevertheless, it would be feasible to attain a considerable reduction of greenhouse gas emissions to the atmosphere derived from this activity capturing the $CO_2$ produced by fossil fuels oxidation. The chemical-looping combustion (CLC) technique is based on a chemical intermediate agent which gets oxidized in an air reactor and is then conducted to a separated fuel reactor where it oxidizes the fuel in turn. Thus, the oxidation products $CO_2$ and $H_2O$ are obtained in an output flow in which the only non-condensable gas is $CO_2$, allowing the subsequent sequestration of $CO_2$ without energy penalty. Furthermore, with shrewd configurations a lower exergy destruction in the combustion chemical transformation can be achieved. This paper focus on a Second-Law analysis of a CLC combined cycle power plant with $CO_2$ sequestration using syngas from coal and biomass gasification as fuel. The key thermodynamic parameters are optimized via the exergy method. The proposed power plant configuration is compared with an equivalent gas turbine system based on a conventional combustion, finding a notable increase of the power plant efficiency. Also, the sensitivity of the results to syngas composition is investigated by considering different $H_2$-content fuels.

**Keywords:** chemical-looping combustion; exergy analysis; Second-Law efficiency; efficient system for power generation; carbon capture and storage; gas turbine system; synthesis gas

**PACS classifications:** 88.05.Bc,88.05.De

---

## 1. Introduction

The carbon capture and storage (CCS) is seen as a potential option for mitigation of the greenhouse gas (GHG) emissions produced by power generation based on fossil fuels combustion. Thus, it could help during the transitional period of development of new and clean sources of energy.

Several separation methods have been proposed *e.g.* chemical absorption or adsorption, separation by membrane or cryogenic separation among others. For instance, [1] describes a capture method via amine chemical absorption in the case of a "post-combustion" strategy. Nevertheless, the high energy penalty involved in the separation of carbon dioxide from a gaseous stream seriously questions the viability of CCS in thermal power plants in practice. Regarding thermochemical gasification of solid fuels, they are decarbonized to a mixture of mainly hydrogen, carbon monoxide and carbon dioxide (synthesis gas or merely syngas). In this case a "pre-combustion" strategy is preferred, since $CO_2$ is quite more concentrated in the syngas than it is in the air after combustion. The energy penalty is lower but still important. Several methods are assessed by [2]. Another interesting option is the "oxy-combustion" strategy, which consists in burning the fuel with pure oxygen instead of with air. Consequently an easy separation of $CO_2$ is obtained by cooling the combustion gases and condensing water. Interesting energy savings strategies have been proposed to reduce the energy cost [3], but still a significant energy consumption takes place in the oxygen separation from air.

The chemical-looping combustion (CLC) is an alternative combustion system proposed by [4]. A lot of research has been carried out and many other contributions have given rise to the progress of this technology. Because of its interest in the field of gas turbines, most studies related to CLC have been devoted to the study of methane as fuel. Other alternative fuels, *e.g.* methanol, also have been suggested and studied [5]. The interest of other fuels is of interest as well. In particular synthesis gas deserves some attention. Previous works [6],[7] give a very interesting insight on CLC systems and a thermodynamic analysis of a syngas fueled gas turbine cycle. A more recent job [8], provides an exhaustive energetic analysis of a syngas fueled combined cycle with CCS from a First-Law point of view. The scope of the present work is to complement that analysis with a Second-Law approach in order to provide a further understanding of such systems. The overall exergetic performance of a CLC combined cycle power plant with integrated $CO_2$ capture and fueled by syngas is studied. Details on the behavior of the proposed power plant in a range of operating conditions are provided. In addition, it has been found of interest to compare the proposed CLC-based system with a conventional gas turbine cycle. Finally, the higher complexity of CLC systems makes them more sensitive to changes in the fuel chemical composition. For this reason, different syngas compositions have been considered and studied.

### *1.1. Chemical-looping combustion: idea and objective*

The CLC concept is presented schematically in Fig. 1. Combustion takes place in two steps by way of an intermediate agent, an oxygen carrier, so that air and fuel never get in contact. Two different reactors are used. In the air reactor (oxidation reactor) the oxygen carrier is oxidized in presence of air. Then, it is transferred to the fuel reactor (reduction reactor) where the oxygen is interchanged: the carrier is reduced and the fuel is oxidized. Finally, the reduced oxygen carrier is redirected again to the air reactor to close the loop. As discussed in section 2.2, the typical oxygen carrier are metal oxides. We denote it

generically by "MeO". In the case of an hydrocarbon an carbon monoxide as fuel, the reactions in the fuel reactor are the following oxidation reactions:

$$(2n + m)\mathrm{MeO} + \mathrm{C}_n\mathrm{H}_{2m} \longrightarrow (2n + m)\mathrm{Me} + m\mathrm{H_2O} + n\mathrm{CO_2} \quad (1)$$

$$\mathrm{MeO} + \mathrm{CO} \longrightarrow \mathrm{Me} + \mathrm{CO_2} \quad (2)$$

As a consequence, the outcome of the fuel reactor is just a mixture of $CO_2$ and $H_2O$. They are not diluted in air, contrarily to a conventional combustion. The only non-condensable gas in the combustion gases is carbon dioxide, allowing an easy separation.

Te loop is closed at the oxidation reactor where the carrier "Me" takes the required oxygen from air in accordance to:

$$\mathrm{Me} + \frac{1}{2}\mathrm{O_2} \longrightarrow \mathrm{MeO} \quad (3)$$

Depleted air is got as a result of this reaction, physically separated from the exhaust gases stream.

**Figure 1.** Scheme of the CLC idea.

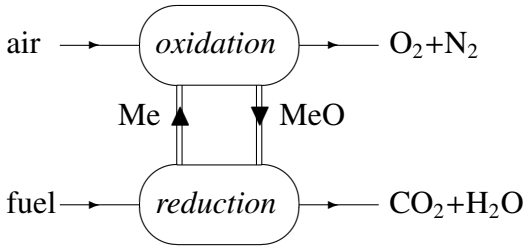


The oxidation reaction (3), it is strongly exothermic in all cases. Nevertheless, it may happen that the reduction reactions (1),(2) are endothermic or exothermic. It depends on both, fuel and oxygen carrier. If it is the case that one of the reduction reactions is endothermic (or perhaps both of them), then it is possible to find an interesting strategy to produce a sort of "chemical exergy amplification". The idea is to enforce the endothermic reaction to occur at low or medium temperature. The required heat consumption could be supplied from a medium temperature heat reservoir. In effect, the Hess' Law imposes that the total heat to be released in the combination of reactions (3) and (1)/(2) equals the fuel's heat of combustion. It follows that the oxidation reaction must release a higher amount of heat than a conventional combustion:

$$\Delta H^\circ_{\mathrm{comb}} = \Delta H^\circ_{\mathrm{red}} + \Delta H^\circ_{\mathrm{oxi}} < 0 \; ; \quad \Delta H^\circ_{\mathrm{red}} > 0 \Rightarrow \left|\Delta H^\circ_{\mathrm{oxi}}\right| > \left|\Delta H^\circ_{\mathrm{comb}}\right|$$

On the other hand, the exergy content of heat increases with the temperature at which it is exchanged[1]. Thus, CLC can be seen as a "chemical heat pump" that takes an energy flow with little exergy content and transforms it into another energy flow that carries a bigger amount of exergy. From a different an complementary point of view, what happens is that the exergy destruction that is related to the irreversibility of the whole chemical transformation is lower in the case of CLC compared with a

[1] This is a very well known result; see for example the exergy balance equation (6) given in a following section of this paper.

conventional combustion. A detailed theoretical analysis of this type of "exergy amplification" is given by [9].

The interesting point is that in the case of a gas turbine system, the gases at turbine outlet can be used as the medium temperature heat source that provides the required heat to the reduction reactor.

In addition, and more importantly, the separation of $CO_2$ generated as a consequence of fuel's oxidation is "energy-free". As described previously, a mixture of mainly carbon dioxide and water is got and a simple condensation of water allows an easy sequestration of $CO_2$. This was the case for the "oxy-combustion" technique mentioned above, but CLC avoids any energy penalty due to both, separation of the carbon dioxide from other gases and also separation of the oxygen from air. The previous two aspects, and particularly the last one, are the major advantages of CLC. Moreover, it may be of interest to remark that the separation of fuel and air into different reactors avoids the existence of flames, leading to less $NO_x$ formation [10].

The CLC reactors shown in Fig. 1 can be materialized in several ways [11]. The approach most frequently proposed are fluidized-bed reactors. The metal oxides are found in the form of fine "floating" particles. The size of particles must be chosen in order to ensure a sufficient contact area to provide optimal conditions for the chemical reactions in both reactors. Catalysis might be necessary to improve the chemical kinetics, but this point is out of the scope of this work.

## 2. Description of the study

### *2.1. Proposed CLC-based gas turbine cycle*

The proposed CLC combined cycle with carbon dioxide sequestration, depicted in Fig. 2, is taken from Ref. [8] and is based on prior ideas suggested by [5] and [6]. A further discussion on the advantages of this configuration can be found in [8]. The thermodynamic parameters of the cycle have been maintained as given by [8]:

- Ambient conditions: 15 °C (288.15 K), 1 atm (101.325 kPa), 60% RH (relative humidity).
- Fuel conditions: 153.4 °C (426.58 K), 27.24 bar.
- Pressure drop at the air filter: 1 kPa.
- Isentropic efficiency of compressors: 0.845.
- Isentropic efficiency of gas turbines: 0.895.
- Pressure drop in reactors: 4%
- Heat losses in reactors: 0.5% in the oxidation reactor, 0.2% in the reduction reactor.
- Pressure drop in HRSG: 3.5%.
- Pressure drop in other heat exchangers: 1%.

- Pinch point in heat exchanges: 10 °C in gas–gas exchanges, 50 °C in the air pre-heater.
- Temperature of exhaust gases after HRSG: dew point and never under 90 °C (363.15 K).
- Final pressure for $CO_2$ storage: 85 bar.

**Figure 2.** CLC-based combined cycle with $CO_2$ sequestration and storage.

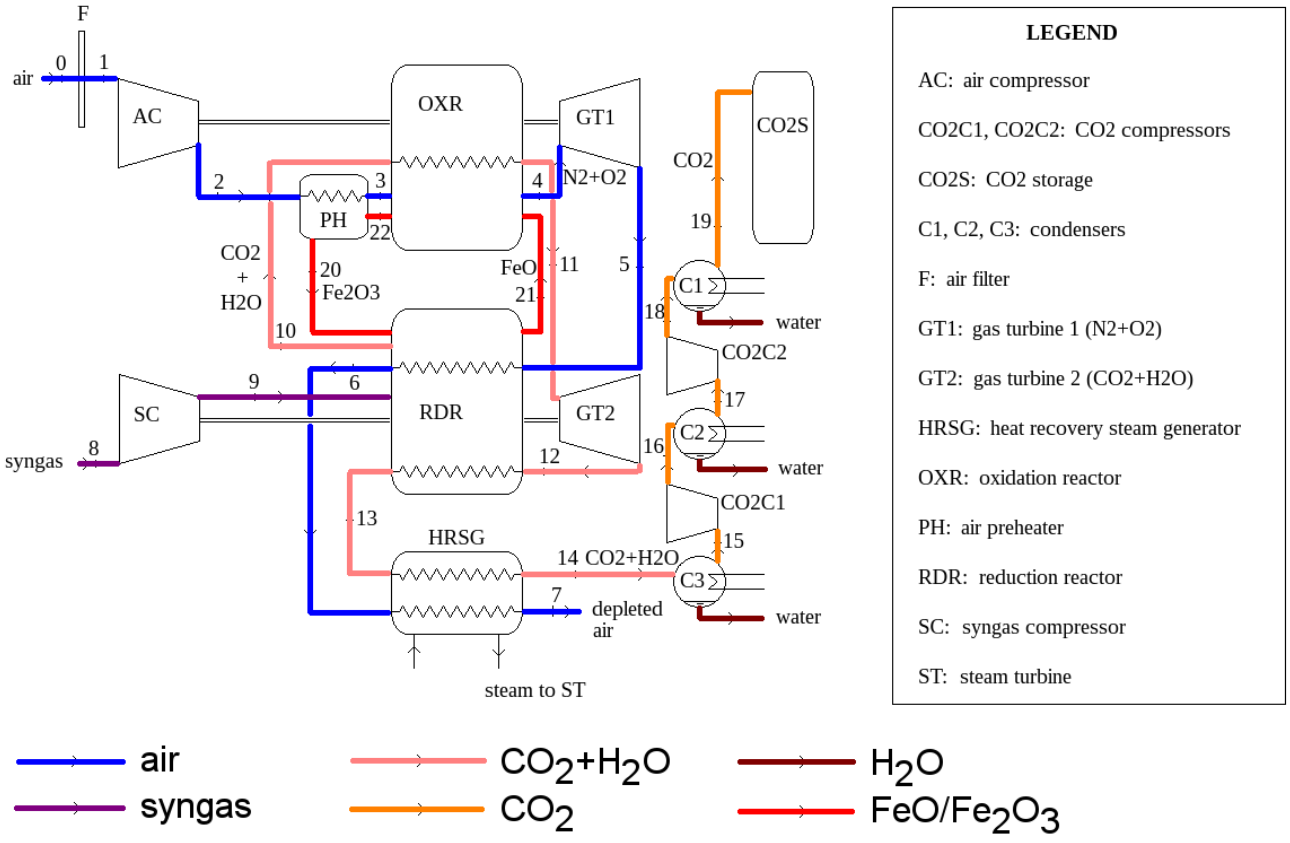


For the steam cycle (not included in Fig. 2) a one-level pressure conventional steam cycle has been considered. Condensation pressure is fixed at 0.07 bar, pressure at the boiler economizer inlet is set to 76 bar and steam pressure at the boiler outlet is 67 bar. The steam temperature at the boiler output is assumed 20 °C lower than the exhaust gas temperature and never higher than 545 °C (818.15 K).

The above values are considered to be reasonable and within the common range in combined cycles [5],[11],[12]. Fuel conditions have been taken from available preliminary data on gasification processes [13]. Regarding the final compression pressure for $CO_2$, it allows transport or storage as a supercritical fluid with high density. The particular figure 85 bar used here is taken from [11]. The compression setup has been modeled to take place in two stages with the same compression ratio, giving:

$$p_{17} = \sqrt{p_{15} p_{18}}$$

The rest of the free parameters of the cycle has been set to their optimal values from the point of view of power production. These optimal values are adjusted as a function of GT1 turbine inlet temperature (TIT) and the reactors pressure ($p_r$).

The overall exergetic performance of the power plant showed in Fig. 2 is evaluated after analysis and optimization.

Finally, the conventional gas turbine cycle shown in Fig. 3 has been simulated as well with the goal of comparing the exergy destruction in the combustion chemical transformation. Equivalent values of isentropic efficiencies of compressors and turbines, heat losses and pressure drops have been adopted.

**Figure 3.** Combined cycle with conventional combustion system.

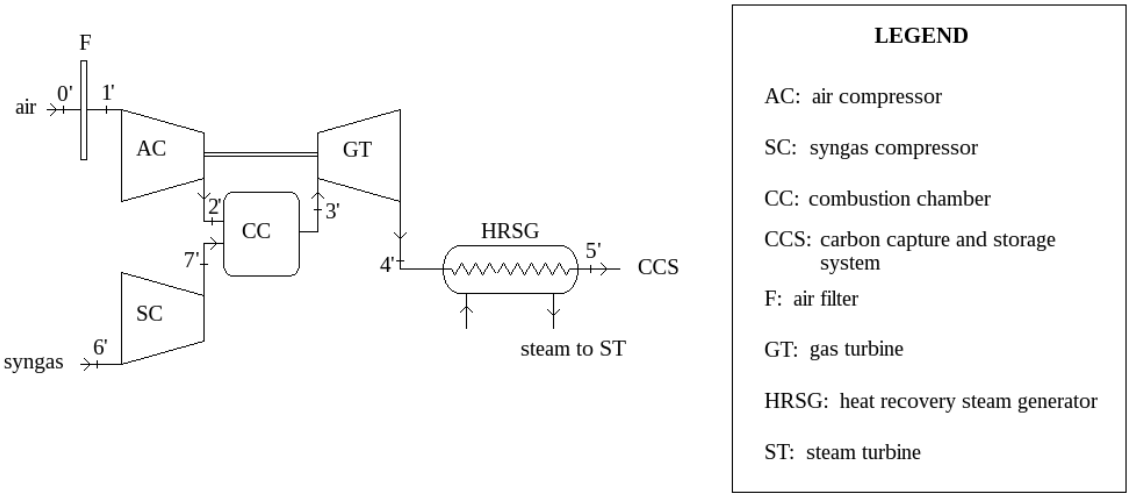


### *2.2. Oxygen carrier*

Many metal oxides have been suggested as oxygen carriers for CLC. When $CH_4$ is used as fuel, some of the most typical of them are the pairs $Fe_2O_3$–$Fe_3O_4$, NiO–Ni, CuO–$Cu_2O$, CuO–Cu and $Mn_2O_3$–$Mn_3O_4$. However, when the fuel is a syngas, the gases to be oxidized are $H_2$ and CO instead of $CH_4$. The only pair among those checked that satisfies the requirement of providing an endothermic reduction reaction is $Fe_2O_3$–FeO:

$$\begin{aligned} Fe_2O_3 + H_2 &\longrightarrow FeO + H_2O \quad ; \quad \Delta H^\circ_{298} = 39.611\ \text{kJ/mol} \\ Fe_2O_3 + CO &\longrightarrow FeO + CO_2 \quad ; \quad \Delta H^\circ_{298} = -1.564\ \text{kJ/mol} \end{aligned} \tag{4}$$

where $\Delta H^\circ_{298}$ represents the standard enthalpy of reaction at 25 °C (298.15 K) and 1 bar. Since an important proportion of $H_2$ is present in syngases, the combined heat of reactions (4) is positive, leading to an oxidation reaction with a heat of reaction higher than the fuel's lower heating value (LHV) as discussed in section 1.1:

$$2FeO + \tfrac{1}{2}O_2 \longrightarrow Fe_2O_3 \quad ; \quad \Delta H^\circ_{298} = -281.438\ \text{kJ/mol} \tag{5}$$

Some reports have pointed out that some amount of inert material might be necessary to ensure that the solid particles behave with the required physical stability against important changes of temperature. Since it is thought [7] that YSZ (yttria-stabilized $ZrO_2$) acts as a catalyst in reactions (4), a mass of 0.27 mol of $ZrO_2$ per mol of FeO has been added to the oxygen carrier streams for this purpose. This amount of inert material is an intermediate value between those proposed in [6] and [11] (0.2 and 0.34 respectively). The $ZrO_2$ merely acts as a heat carrier between the two reactors without taking part in any chemical transformation.

### *2.3. Fuels under study*

As the hydrogen content of fuel increases, additional amount of heat is required in order to enforce the first of the reduction equations (4). The heat balances and also the thermodynamic equilibrium in CLC reactors is considerably influenced by the fuel composition. In order to quantify the impact of the hydrogen content on the CLC performance three different syngas compositions have been tried. Tab. 1 gives the exact composition of each syngas under study together with their LHV and standard chemical exergy. Since the exergetic approach is intended along this paper, the fuel's chemical exergy will be taken as reference for the quantification of the power plant efficiency instead of its LHV, as discussed in a later section.

**Table 1.** Composition in mole fraction, LHV and chemical exergy of considered fuels.

| Fuel | Substrate | CO (%) | $H_2$ (%) | $CO_2$ (%) | $N_2$ (%) | Ar (%) | $H_2O$ (%) | LHV (kJ/mol) | $e_{CH}$ (kJ/mol) |
|---|---|---|---|---|---|---|---|---|---|
| Syngas A | wood waste | 46.90 | 26.02 | 18.45 | 8.09 | 0.52 | 0.02 | 195.64 | 200.70 |
| Syngas B | miscanthus | 45.84 | 35.46 | 11.28 | 7.12 | 0.28 | 0.02 | 215.47 | 219.00 |
| Syngas C | Pittsburgh n8 | 63.77 | 29.65 | 4.25 | 1.78 | 0.53 | 0.02 | 252.16 | 253.81 |

Syngas A and B are obtained from thermochemical gasification of biomass substrates, wood waste and miscanthus (a herbaceous energy crop) respectively. Rather, the one called syngas C comes from the gasification of an American coal, "Pittsburgh n8". The first two present a significantly different amount of hydrogen and the third one has an intermediate value between them and at the same time gives an example of a quite different amount of carbon monoxide. The rest of the syngas components (others than $H_2$ and CO) do not take part in the involved chemical reactions but they might influence the chemical equilibrium eventually reached.

### *2.4. The exergy method*

The limit of First-Law analysis is that it does not account for energy quality. However, we know from the Second Law that many energetic transformations occur only in one way and not in the opposite. For instance, converting from mechanical to thermal energy is an easy straight ahead process while the opposite is quite complex. Therefore, not all energy flows can be said to poses the same capability to induce a desired effect, and the concept of exergy arises in order to quantify that capability. A common definition of exergy would state that *"exergy is the maximum theoretical useful work obtainable as the system interact to equilibrium, heat transfer occurring only with the environment"*. The exergy method allows to compare the actual performance of systems and processes with the best that could be obtained in accordance with the impositions from not only the First Law, but also from the Second Law. Therefore it makes possible to detect and quantify the possibilities of improving thermal and chemical processes and systems.

The expression of the exergy balance in an open system that describes a stationary process is given by:

$$\sum_{i \in \text{outputs}} \dot{n}_i e_i - \sum_{i \in \text{inputs}} \dot{n}_i e_i = (\dot{Q} - T_0 \dot{J}_s) - \dot{W} - \dot{I} \tag{6}$$

where

- $\dot{n}$ is the molar flow rate of a stream,
- $e$ is the thermodynamic function of state *flow exergy*,
- $\dot{Q}$ is the heat flow rate exchanged by the system,
- $\dot{J}_s$ is the entropy change rate associated with heat flow. For a single temperature system: $\dot{J}_s = \int \frac{đ\dot{Q}}{T}$; for a multi-temperature system: $\dot{J}_s = \sum_k \int \frac{đ\dot{Q}_k}{T_k}$.
- $\dot{W}$ is the mechanical power extracted from the system,
- $\dot{I}$ is the exergy destruction rate due to internal irreversibilities.

When a particular system exchanges heat that cannot be useful for a given purpose, *i.e.* the heat exchanges are merely heat losses to the environment, the heat flow terms in (6) can be included together with the exergy destruction rate term in a total exergy loss rate term:

$$\dot{I}_\text{t} = \dot{I} - (\dot{Q} - T_0 \dot{J}_s)$$

Including this in the exergy balance:

$$\sum_{i \in \text{outputs}} \dot{n}_i e_i - \sum_{i \in \text{inputs}} \dot{n}_i e_i = -\dot{W} - \dot{I}_\text{t} \tag{7}$$

The flow exergy function $e$ represents the work per mol of substance that could be obtained from a stream as the system comes to equilibrium whit the environment, involving any auxiliary devices. Every imbalance between a stream and the environment may result in additional work to be generated. In general, the flow exergy is usually split in two terms:

- The so-called *physical exergy* involves thermal and mechanical imbalances with the environment. Disregarding kinetic and potential energy, this term can be shown to be equal to:

  $$e_\text{PH} = (h - h_0) - T_0(s - s_0) \tag{8}$$

  As usual, $h$ and $s$ are the molar enthalpy and entropy of the stream respectively at its current temperature and pressure. The subscript '0' represents the inert state, *i.e.* the referred thermodynamic function is evaluated considering that stream at ambient temperature and pressure.

- The so-called *chemical exergy* involves diffusive and chemical imbalances with the environment. The process by which equilibrium would be attained should happen at constant temperature equal to $T_0$ (ambient temperature). It can be shown that the maximum theoretical work per mol of substance produced in such a process is the opposite to the change of the specific Gibbs function:

  $$w_{T_0}^\text{max} = -\Delta g$$

  For a pure substance this can also be split into two terms:

– The first one represents the change of the Gibbs function per mol of substance that happens in a degradation chemical transformation until chemical equilibrium with the environment:

$$\Delta g^{(1)} = \Delta G^{\circ}_{\text{deg}}$$

For instance, in the case of a fuel, this would be referred to the combustion reaction. In the case of substances present in the atmosphere in the same form, this term would not exist, *e.g.* nitrogen, oxygen, carbon dioxide, water, *etc*.

– Since this degradation chemical reaction should occur considering that the involved reactive and products are taken from or given to the environment in a manner that the diffusive equilibrium is also satisfied, a second term is needed to account for the change of the Gibbs function per mol of substance required for the chemical potentials of the substances to get equal to their actual values in the environment:

$$\Delta g^{(2)} = \sum_j \nu_j^{\text{deg}} \left( \mu_j^{\text{env}} - \mu_j^{\text{pure}}(T_0, P_0) \right)$$

where $P_0$ is the ambient pressure, $\mu_j$ represents the chemical potential of substance $j$ involved in the degradation reaction (in pure form or its actual value in the environment) and $\nu_j^{\text{deg}}$ denotes the stoichiometric coefficient of substance $j$ in that reaction. For the case of gases, usually the atmosphere is considered to behave as an ideal gas mixture, giving $\mu_j^{\text{env}} - \mu_j^{\text{pure}}(T_0, P_0) = RT_0 \ln x_j^{\text{atm}}$, where $x_j^{\text{atm}}$ is the mole fraction of gas $j$ in the atmosphere. As an example, for the case of methane, the degradation reaction would be the combustion $CH_4 + 2O_2 \rightarrow 2H_2O + CO_2$ (with $\nu_{O_2}^{\text{deg}} = -2$, $\nu_{H_2O}^{\text{deg}} = +2$, $\nu_{CO_2}^{\text{deg}} = +1$), and:

$$\Delta g^{(2)} = RT_0 \ln \frac{\left(x_{H_2O}^{\text{atm}}\right)^2 x_{CO_2}^{\text{atm}}}{\left(x_{O_2}^{\text{atm}}\right)^2}$$

Thus, the chemical exergy of a pure substance is calculated as:

$$e_{\text{CH}} = -\Delta G^{\circ}_{\text{deg}} - \sum_j \nu_j^{\text{deg}} \left( \mu_j^{\text{env}} - \mu_j^{\text{pure}}(T_0, P_0) \right) \tag{9}$$

There are several sources that tabulate standard chemical exergy of pure substances. In this work we base the calculations in the values given by [14].

Finally, for a mixture of substances, the chemical exergy could be calculated as the average chemical exergy of the individual components taking part, plus and additional term that accounts for the change of the specific Gibbs function associated with the separation of the mixture into its components in pure form at ambient temperature and pressure. Considering a mixture with $C$ components this would be:

$$e_{\text{CH}} = g^{\text{M}} + \sum_{j=1}^{C} x_j e_{\text{CH},j} \tag{10}$$

where $x_j$ is the mole fraction of the component $j$ in the mixture. If it can be seen as an ideal Lewis-Randall mixture, the specific mixing Gibbs function is given by $g^{\text{M}} = RT_0 \sum_j x_j \ln x_j$.

Defining for every stream $\dot{E}_i = \dot{n}_i\,(e_{\mathrm{PH}} + e_{\mathrm{CH}})_i$, the exergy balance can be reordered as follows:

$$\sum_{i\,\in\,\text{inputs}} \dot{E}_i = \sum_{i\,\in\,\text{outputs}} \dot{E}_i + \dot{W} + \dot{I}_{\mathrm{t}} \tag{11}$$

This exergy balance equation can be used to calculate the total exergy loss in a whole thermodynamic cycle, but also and more interestingly, for each component individually. In this way it is possible to detect the points of the cycle with a bad performance from a "combined-First&Second-Laws" point of view, arising the possibility of improving thermal and chemical processes and systems.

### *2.5. Simulation methodology*

The simulation of the CLC-based combined cycle power plant shown in Fig. 2 has been carried out relying on the PATITUG library, an own software for thermodynamic analysis developed by the Applied Thermodynamics Group of the Technical University of Madrid. The PATITUG library contains a number of modules for the representation of each component of the cycle, and conveniently assembled allows a complete thermodynamic evaluation of the ensemble based on mass, energy and exergy balances. Several equations of state for gaseous pure substances are available for the calculation of thermodynamic properties depending on the conditions, providing an accurate thermodynamic characterization of every stream of the cycle. More information on PATITUG capabilities are given by Refs. [12],[15].

### *2.6. Thermodynamic modeling*

We give here a brief summary of the thermodynamic assumptions. A much more detailed description on the thermodynamic modeling of the proposed CLC system can be found in [8]. Regarding gaseous substances, the following equations of state have been applied:

a) For water:

- Above the boiling temperature of water at a given pressure, IAPWS-IF97 equation of state is used.
- Below the boiling temperature, water in gaseous state is still found as far as the partial pressure of water in the gaseous mixture maintains below the vapor pressure at that temperature. For this case, the virial gas equation of state truncated after the second term is used.

b) For non-condensable gases:

- For a specific volume close to the critical specific volume and supercritical fluids the Lee-Kesler's equation of state is applied.
- For the rest of the cases the virial gas equation of state truncated after the second term is used.

For solids, correlations for specific enthalpy and entropy dependence with temperature taken from the NIST Chemistry Webbook [16] with small corrections have been applied.

Thermochemical data such as standard heat of formation and standard molar entropy has been taken from [17], while the standard chemical exergy values have been read from [14] for all substances.

## 3. Results and discussion

### *3.1. Chemical equilibrium*

It is implicitly assumed that the required reaction times in relation to the chemical kinetics are ensured. The conversion of fuel into the oxidation products $CO_2$ and $H_2O$ is then subject to the chemical equilibrium constraint:

$$K_a(T) = \exp\left(-\frac{\Delta G^\circ(T)}{RT}\right) \tag{12}$$

where $\Delta G^\circ(T)$ is the standard Gibbs' function of reaction as a function of temperature. $K_a$ is the equilibrium constant of the chemical reaction, which depends on the composition of the reactive mixture. Equation (12) is used to determine the composition at equilibrium.

Results on the conversion ratio (CR) of fuels are presented in Fig. 4, where CR is defined as the fraction of the initial quantity of a particular fuel that gets oxidized at equilibrium conditions. As the initial amount of water in the fuels under study is almost zero, the curves for hydrogen's CR are indistinguishable for the three fuels. The influence of pressure on CR is very slight since the number of moles is conserved in both reactions (4).

**Figure 4.** Hydrogen and carbon monoxide conversion ratios at 15 bar as a function of temperature.

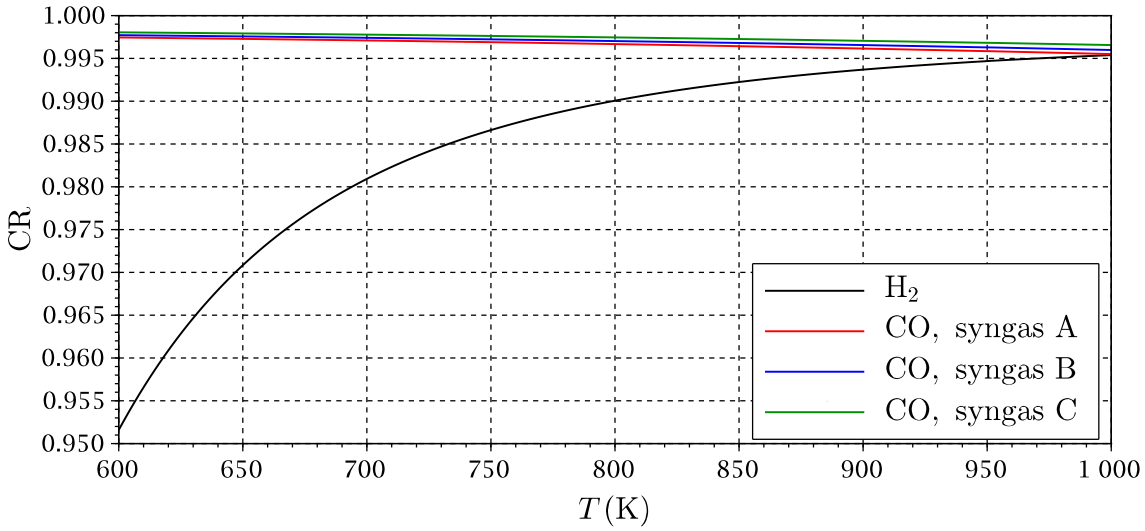


The conversion ratio of hydrogen increases with temperature, in accordance with Le Châtelier's Principle, since the first reaction of (4) is endothermic. In the case of carbon monoxide, it can be observed a minor decrease with temperature (the second reaction of (4) is slightly exothermic) and is somewhat higher for the fuels with a lower content of carbon dioxide, as this has a certain influence in the equilibrium condition. Unlike with conventional combustion, the fuel cannot be completely converted due to the equilibrium restrictions, but Fig. 4 shows that for temperatures of the order of 800 K, hydrogen's CR becomes $\sim$99% while carbon monoxide's CR reaches 99.7 – 99.8% for all fuels. Thus, at this temperature only about 0.55% of the syngas' initial chemical exergy would be wasted as

a result of incomplete oxidation. Nevertheless, the exergy savings associated with the "chemical heat pump" effect counterbalances more than enough this exergy loss, as discussed in section. 3.4.

With respect to the oxidation reactor, it has been found that the chemical equilibrium fails to occur, as it would be obtained for a very small mole fraction of oxygen, far below the amount of oxygen available in the reactor.

### *3.2. Optimization of cycle parameters and exergy efficiency*

The thermodynamic working conditions of the CLC cycle represented in Fig. 2 are defined by a small set of parameters. The overall governing parameters are the main gas turbine (GT1) TIT (which also is the temperature of the oxidation reactor) and the reactors pressure $p_r$.

There is a degree of freedom about the reduction reactor temperature $T_{red}$. This is the key parameter to be determined by optimization, considering the opposite factors involved. As discussed previously the hydrogen's CR increases with temperature. However, taking into account that the required heat to enforce this reaction is taken from the gas turbines outlet streams, it is clear that this temperature is bounded above. An iterative algorithm has been implemented to calculate $T_{red}$ as the highest temperature possible that allows to satisfy the energy balance in the reduction reactor.

There is a second degree of freedom of low importance in relation with the expansion pressure at GT2 outlet (stream 12). Calculations show that the pressure that gives the best ratio of power developed by gas turbine GT2 to power consumed by the $CO_2$ reactors is very close to 1.5 bar for all fuels, but the influence in the results is minor in a quite broad range.

The cycle performance is evaluated from an exergetic point of view. The exergy efficiency is given by

$$\eta_{ex} = \frac{\dot{W}_{GT1} + \dot{W}_{GT2} + \dot{W}_{ST} + \dot{W}_{CO_2}}{\dot{E}_{fuel}} \tag{13}$$

$\dot{W}_{GT1}$ is the power generated by GT1, subtracted the air compressor power consumption, $\dot{W}_{GT2}$ is the power generated by GT2 minus the fuel compressor consumption, $\dot{W}_{ST}$ is the power produced by the steam turbine and $\dot{W}_{CO_2}$ is the power consumption of both $CO_2$ compressors:

$$\dot{W}_{GT1} = \eta_{em}(h_1 - h_2 + h_4 - h_5) \quad ; \quad \dot{W}_{GT2} = \eta_{em}(h_8 - h_9 + h_{11} - h_{12}) \quad ; \quad \dot{W}_{CO_2} = (h_{15} - h_{16} + h_{17} - h_{18})$$

A electromechanical efficiency for gas turbine ensembles of $\eta_{em} = 0.98$ has been considered. $\dot{W}_{ST}$ is calculated in a similar way.

A bunch of simulations for different TIT in a range going from 1400 to 1600 K and $p_r$ from 12 to 28 bar has been carried out. For each considered fuel and for every pair of values of TIT and $p_r$ the optimal reduction temperature and the exergy efficiency of the cycle have been obtained. Results are given in Figs. 5 to 10.

It might be interesting to expand on the freaky thermodynamic behavior revealed by these figures. It is observed a change in the tendency of the optimal temperature of the reduction reaction with $p_r$ for a given TIT. In principle, to increase the pressure ratio makes the gas turbines outlet temperature after expansion go down. For this reason, at low pressure ratios the $T_{red}^{opt}$ is reduced with a pressure ratio increase so that the reactor is able to take sufficient heat from the exhaust gas streams outgoing the turbines to satisfy the energy balance. However, there is another opposing effect. The increment of pressure ratio compression

**Figure 5.** Exergy efficiency of CLC cycle for syngas A as fuel.

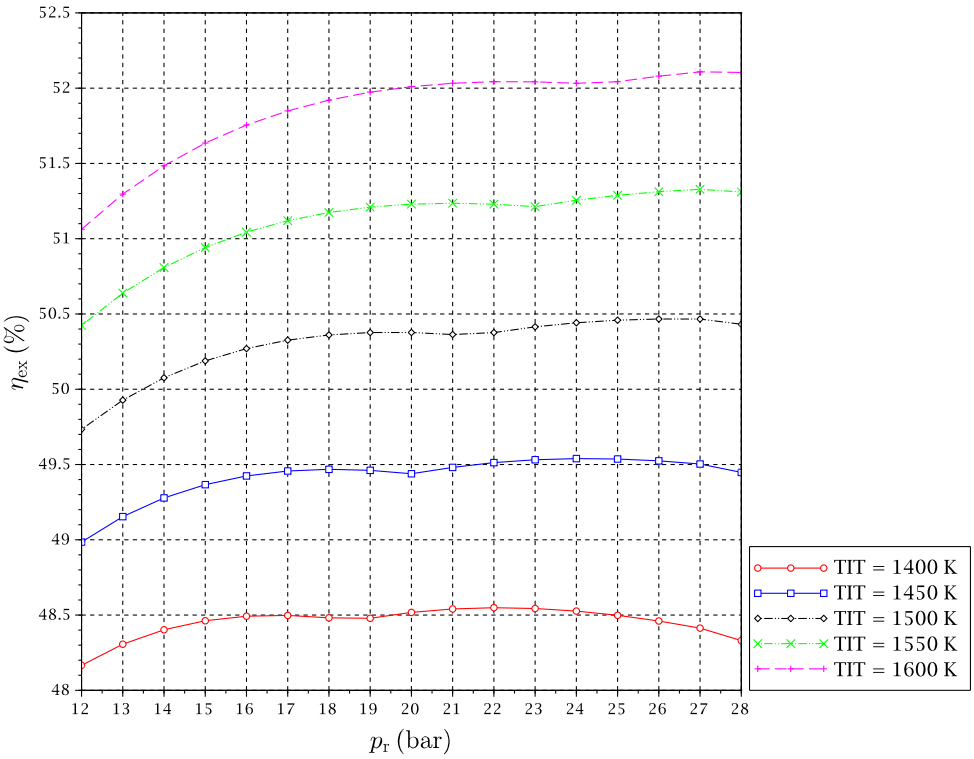


**Figure 6.** Exergy efficiency of CLC cycle for syngas B as fuel.

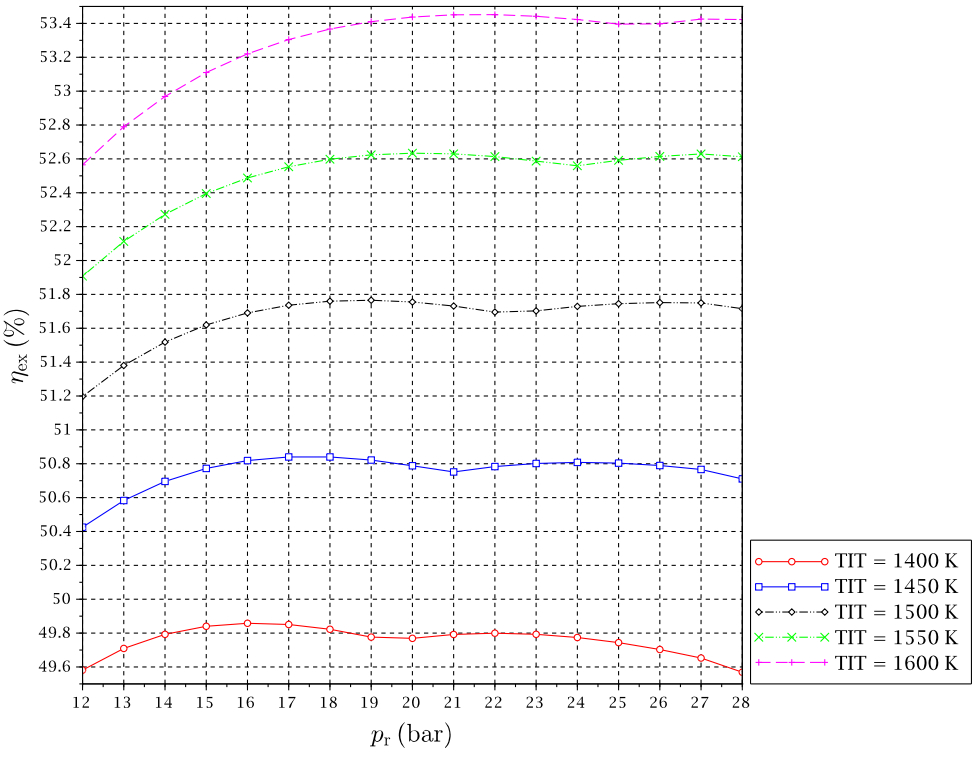

**Figure 7.** Exergy efficiency of CLC cycle for syngas C as fuel.

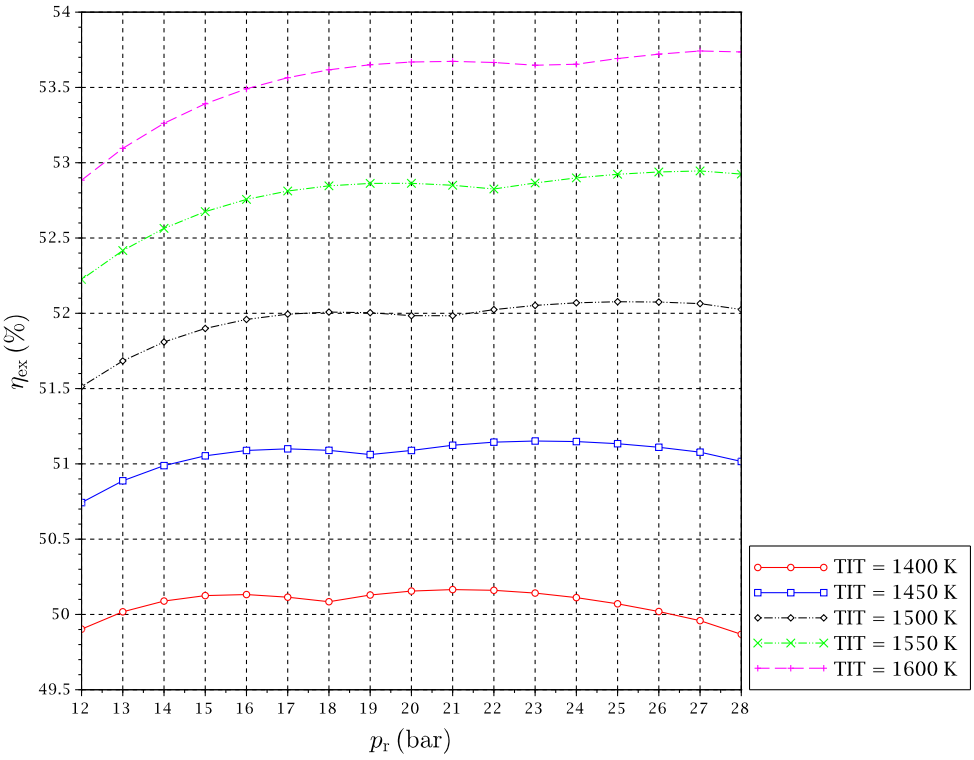


**Figure 8.** Optimal reduction temperature for syngas A as fuel.

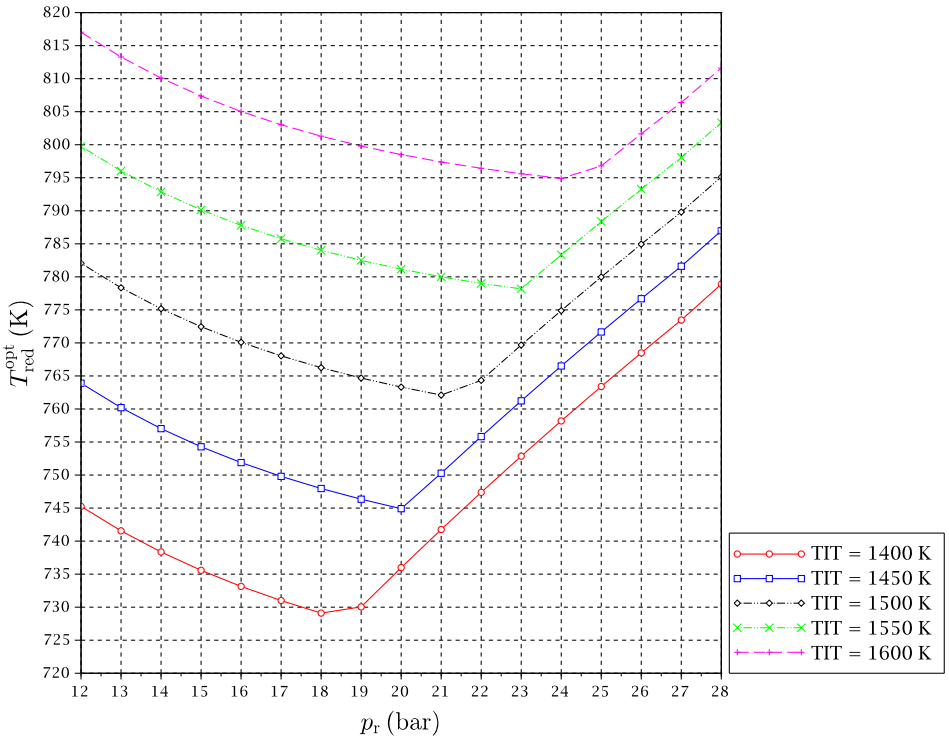

**Figure 9.** Optimal reduction temperature for syngas B as fuel.

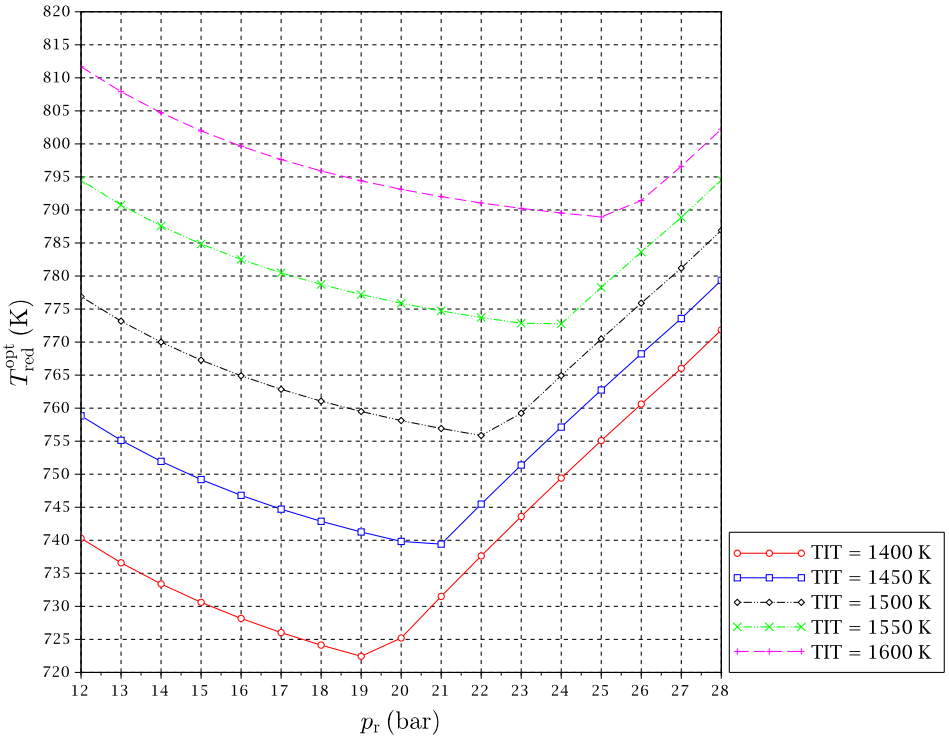


**Figure 10.** Optimal reduction temperature for syngas C as fuel.

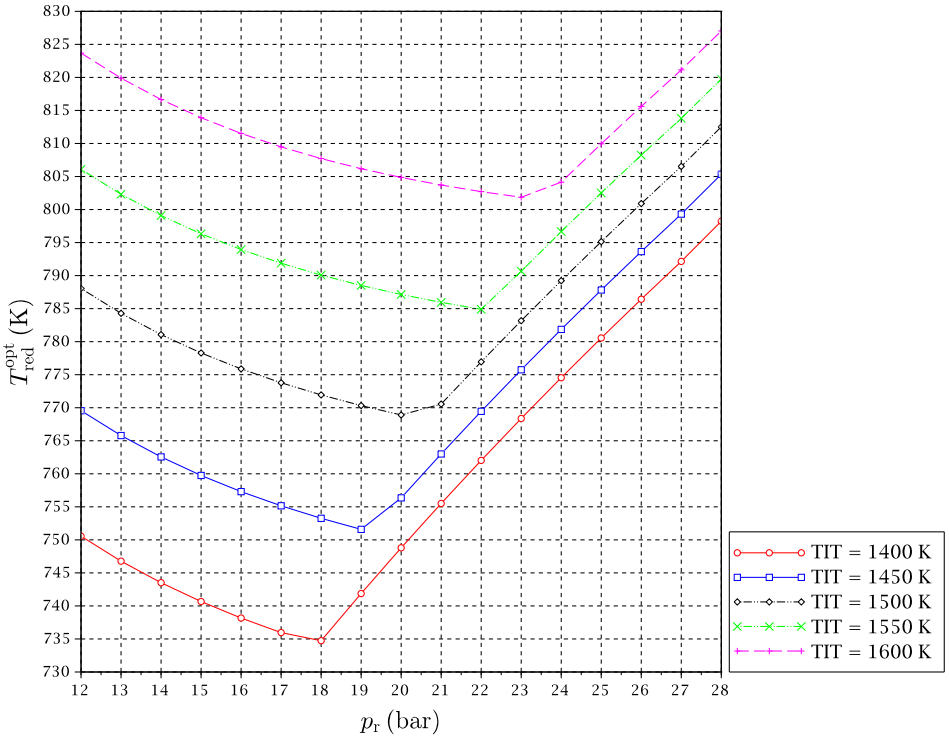

leads to higher temperatures at the compressors outlets, what implies that the inputs to the reduction reactor are received there at higher temperatures. In summary, the following two effects occur at the same time when the reactors pressure is increased:

a) Lower temperature of gas streams at the outlet of the gas turbines.

b) A decrease of heat demand in the reduction reactor.

At some point, b)-effect begins to dominate against a)-effect. At a particular pressure the heat needed by the reactor is decreased to a point that it can be provided by the $CO_2$ + $H_2O$ stream only: the air stream results to uncouple from the reduction reactor heating. This can be seen somehow as a typical "power heat pump" effect[2]. Due to the complex heat coupling of streams and reactors in the CLC cycle, this allows $T_{red}$ to reverse its trend and it begins to increase with pressure ratio (Figs. 8 to 10). We will refer to this point of tendency change as *reduction reactor heating uncoupling point (RRHUP)*. This phenomenon is also revealed in the thermal efficiency plots. Instead of the usual curves with a maximum that are found for a conventional combined cycle, curves with two local maxima of quite similar values are got for this CLC system (Figs. 5 to 7). Consequently a good thermal efficiency almost constant is achieved along a quite wide range of pressure ratios. Tab. 2 shows the position of the exergy efficiency maximum found for each TIT curve (the highest of both), together with the optimal reduction temperatures for these maxima.

**Table 2.** Optimal conditions and maximal exergy efficiencies.

| | Syngas A | | | Syngas B | | | Syngas C | | |
|---|---|---|---|---|---|---|---|---|---|
| TIT | $p_r^{opt}$ | $T_{red}^{opt}$ | $\eta_{ex}^{max}$ | $p_r^{opt}$ | $T_{red}^{opt}$ | $\eta_{ex}^{max}$ | $p_r^{opt}$ | $T_{red}^{opt}$ | $\eta_{ex}^{max}$ |
| (K) | (bar) | (K) | (%) | (bar) | (K) | (%) | (bar) | (K) | (%) |
| 1400 | 22 | 747.9 | 48.55 | 16 | 728.2 | 49.86 | 22 | 762.0 | 50.16 |
| 1450 | 24 | 766.5 | 49.54 | 18 | 742.9 | 50.84 | 23 | 775.7 | 51.15 |
| 1500 | 26 | 784.9 | 50.47 | 19 | 759.5 | 51.76 | 25 | 795.1 | 52.08 |
| 1550 | 27 | 798.1 | 51.33 | 20 | 775.9 | 52.63 | 27 | 813.8 | 52.95 |
| 1600 | 27 | 806.4 | 52.11 | 22 | 791.0 | 53.45 | 27 | 821.1 | 53.74 |

It can be noticed that syngas B presents a higher exergetic efficiency and lower reduction temperature than syngas A. This is justified in base of the different hydrogen content of both syngases. The more hydrogen implies the more needs of heat at the reactors and temperature must be lowered to satisfy the energy balance. In addition, the "chemical heat pump" effect leads to a higher exergy efficiency. Syngas C has an intermediate content of hydrogen but also a significant extra amount of carbon monoxide. Since the oxidation of carbon monoxide is slightly exothermic, the reduction temperature can be increased a

[2] Do not confuse this effect with the so-called "chemical heat pump" effect discussed in section 1.1. The "power heat pump" effect is referred just to the comeback of the energy that was introduced in the cycle as mechanical power in the air compressor as heat provided to the reduction reactor. The exergy content of this heat flow is then amplified by the "chemical heat pump" effect.

bit and the exergy efficiency obtained is consequently the highest of the three fuels under study. Another interesting point is that for the case of syngas B, the highest maximum is the left one, *i.e.* at lower $p_r$, while for syngases A and C the highest maximum is the right one, *i.e.* at higher $p_r$. In any case, the difference in the exergy efficiency between syngases B and C is very slight.

### *3.3. Exergy balances*

Fig. 11 illustrates the exergy flows in the proposed CLC power plant. The exergy input to the power plant is fuel's exergy, mainly the chemical exergy term but also the physical exergy term. The exergy outputs are the compressed $CO_2$ stream and the flue air stream. The exergy content of the latest of both is as a matter of fact a non-recoverable exergy term, so it could be considered as an exergy loss somehow. Another part of the fuel's exergy content is transformed to power in the gas turbine cycle and in the steam cycle. Some of this power must be reinjected to the cycle as the power consumption of $CO_2$ compressors. Finally, the rest of the fuel's exergy content is lost, due to irreversibilities in the cycle and heat losses to the environment.

**Figure 11.** Exergy balances of the CLC cycle with $CO_2$ sequestration.

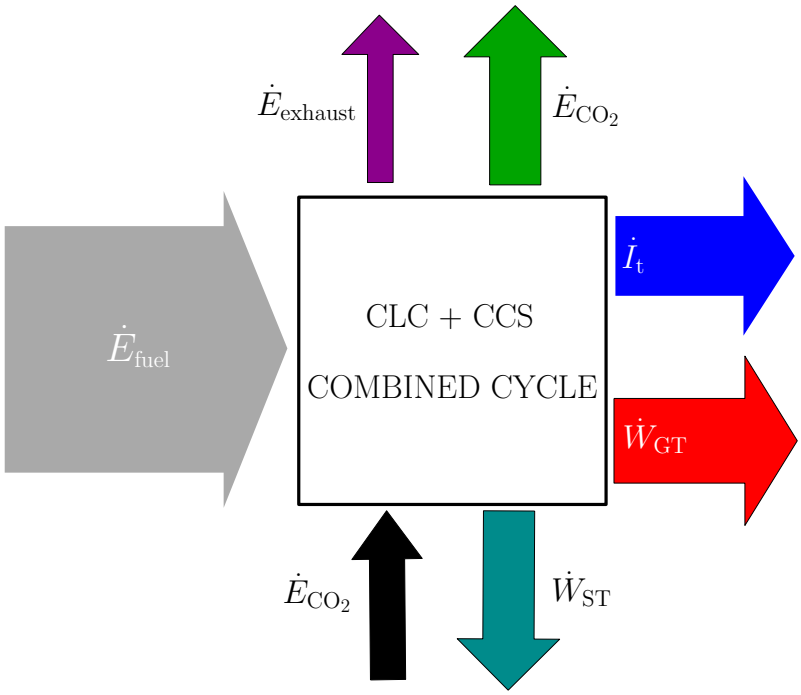


A quantification of the exergy distribution is shown in Tab. 3 for a particular case with TIT = 1550 K, under the optimal conditions for each syngas, given in Tab. 2. Values are given as a fraction of the exergy input to the cycle, *i.e.* normalized by $\dot{E}_{\text{fuel}}$.

It may be of interest to remark the influence of the $CO_2$ compression power consumption in the exergy efficiency of the cycle. The difference between syngases A and C is of about 1.4 percentage points, much more significant that the influence of power generation by gas turbines and steam turbines, and it would be higher if the storage pressure of $CO_2$ were increased. This term can be seen as approximately proportional to the carbon plus inert gases content of syngas (mass flow to be compressed per mol of

**Table 3.** Exergy balances of the whole CLC cycle for TIT = 1550 K and optimal conditions.

| Fuel | $\dot{E}_{CO_2}$ (%) | $\dot{E}_{exhaust}$ (%) | $\dot{W}_{GT}$ (%) | $\dot{W}_{ST}$ (%) | $\dot{W}_{CO_2}$ (%) | $\dot{I}_t$ (%) |
|---|---|---|---|---|---|---|
| Syngas A | 10.07 | 1.20 | 39.82 | 16.99 | -5.49 | 37.41 |
| Syngas B | 8.25 | 1.20 | 39.54 | 17.49 | -4.40 | 37.92 |
| Syngas C | 8.17 | 1.29 | 39.54 | 17.50 | -4.09 | 37.59 |

fuel) and approximately inversely proportional to the fuels chemical exergy. This could be characterized by a fuel dependent carbon&inert/exergy parameter:

$$\text{C\&I/Ex} = \frac{x_{CO} + x_{CO_2} + x_{N_2} + x_{Ar}}{e_{CH}} \tag{14}$$

that can be obtained from Tab. 1 for the fuels under study:

| | Syngas A | Syngas B | Syngas C |
|---|---|---|---|
| C&I/Ex (mol/MJ) : | 3.685 | 2.946 | 2.771 |

and is more or less proportional to the $\dot{W}_{CO_2}$ values given in Tab. 3.

It is also interesting to analyze the dependence of the main exergy flows with the operating conditions. A negligible dependence is found for the exergy content of flue air, $CO_2$ compression power and stored $CO_2$ flow, since their conditions are more or less uncoupled with the rest of the cycle. The exergy flows of total exergy loss, gas turbines power production and steam turbine power production as a function of pressure ratio has been plotted in Figs. 12, 13 and 14 for a particular value of TIT. Values are given as a fraction of $\dot{E}_{fuel}$.

All the Figs. from 12 to 14 show clearly the abrupt change of tendency associated with the RRHUP. In particular Fig. 13 reproduces how an important extra amount of power is produced by GT1 when the reduction temperature begins to increase as the RRHUP is reached due to the combination of the "power heat pump" and "chemical heat pump" effects mentioned previously. This is partially compensated by the lower power produced by the steam cycle (Fig. 14), since the temperature of the air stream entering the HRSG decreases quickly with pressure ratio. However the combination of both effects and a low total exergy loss (Fig. 12), allows to obtain a second maximum in the overall exergy efficiency in a zone of higher pressure ratios (see Figs. 5 to 7).

A more detailed exergy analysis is often presented in the form of a Grassmann diagram. This kind of charts reproduce the exergy flows associated with the different streams connecting the different components of the cycle. Also mechanical power input or output in every component is shown, and the exergy loss is indicated as a decrease in the exergy flow out of the component. In this way, the displayed graphical information allows to identify easily the components with large exergy destruction. We present in Figs. 15 and 16 Grassmann diagrams for two cases: syngas B and syngas C under optimal conditions for TIT = 1550 K. With the aim of facilitating the interpretation of the figures, we remark that the exergy inputs are represented on the left side and the exergy outputs on the right side of each component.

The main differences between both cases can be summarized as follows:

- The optimal pressure for syngas B is 20 bar and for syngas C is 27 bar. As mentioned previously, this is related to the fact that for syngas B the optimal point is reached at pressures lower than

**Figure 12.** Total exergy loss in CLC cycle for TIT = 1550 K.

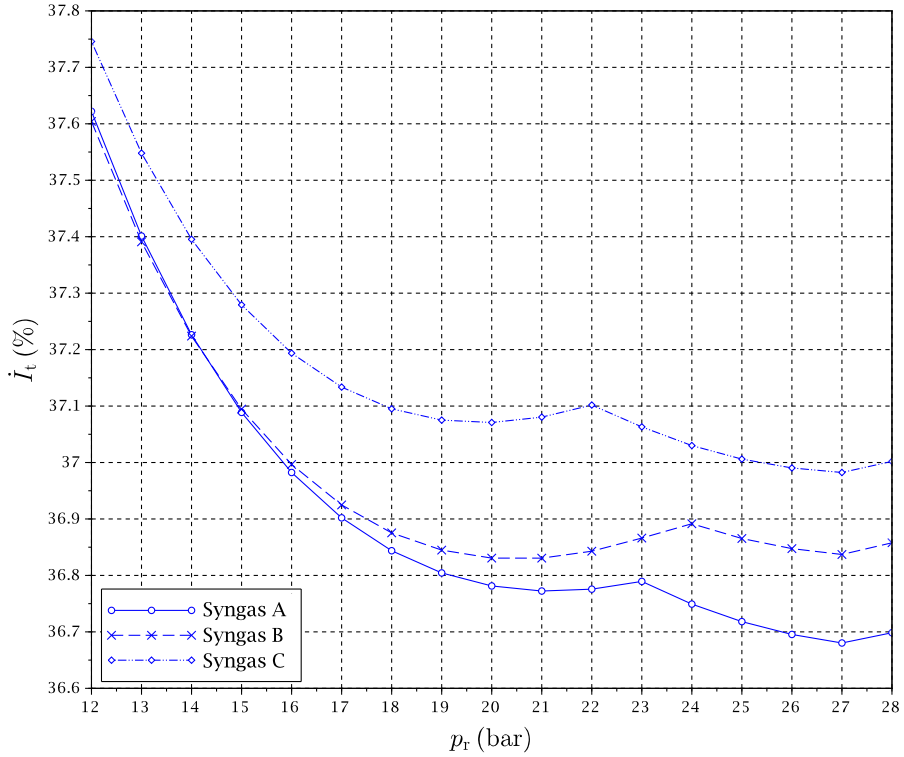


**Figure 13.** Power generated by gas turbines in CLC cycle for TIT = 1550 K.

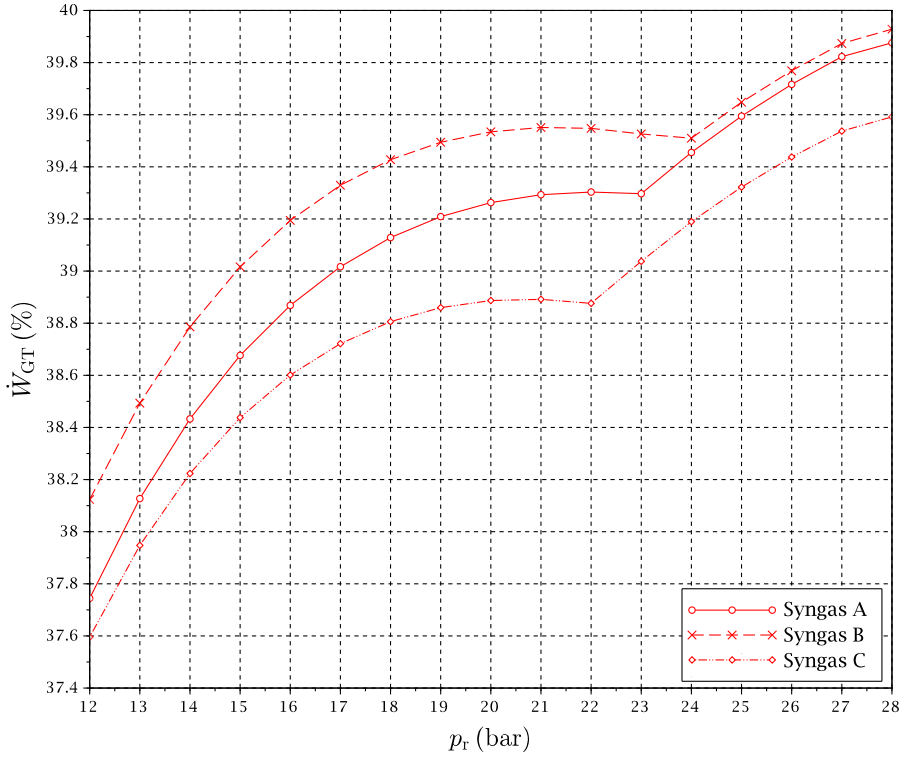

**Figure 14.** Power generated by steam turbine in CLC cycle for TIT = 1550 K.

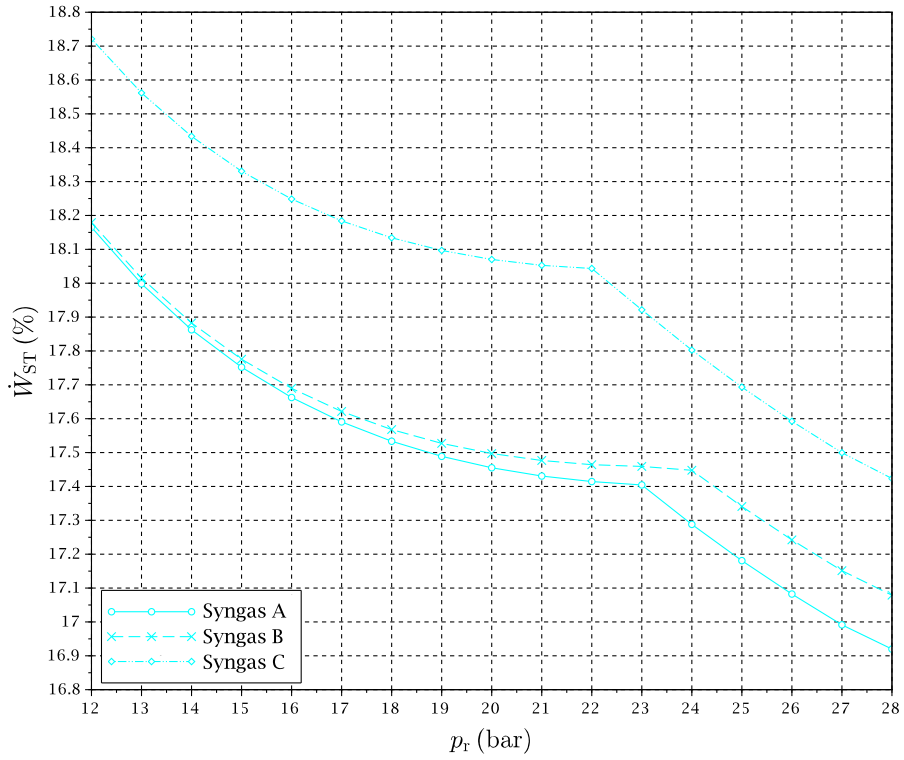


the RRHUP and for syngas C the optimal point is found at higher pressures. This is reflected in higher compression power, higher flow exergy of air and oxygen carrier streams, and higher power production in gas turbine GT1 for the case of syngas C.

- The exergy destruction in the "syngas compressor" is very small for the case of syngas C. Actually, since fuel admission pressure has been set at 27.24 bar, as a matter of fact the "syngas compressor" is acting merely as an isenthalpic pressure loss instead of a compression in both cases represented here. However, the pressure loss is very small for the case of syngas C (down to 27 bar) and somewhat larger for syngas B (down to 20 bar).

For the steam cycle block and the $CO_2$ sequestration module the results are very close to each other.

### *3.4. Comparison with a conventional gas turbine cycle*

In order to illustrate the important differences regarding the exergetic behavior between a CLC gas turbine system and a conventional gas turbine system we have carried out a comparison of the exergy flows of this part of the cycle. Tab. 4 compares the following exergy flows for a reference case of TIT = 1550 K and $p_r$ = 20 bar: the exergy flow of the exhaust gases stream before entering the HRSG, the power generated by the gas turbine block, the exergy loss in the combustion chamber and the exergy losses in the rest of the cycle, all of them given as a fraction of the fuels exergy.

It can be noticed that the exergy destruction in the combustion chamber is of the order of 5 percentage points lower for the CLC cycle. This quantifies the "chemical heat pump" effect in therms of exergy

**Figure 15.** Grassmann diagram for syngas B. TIT = 1550 K, $p_r$ = 20 bar, $T_{red}$ = 776 K.

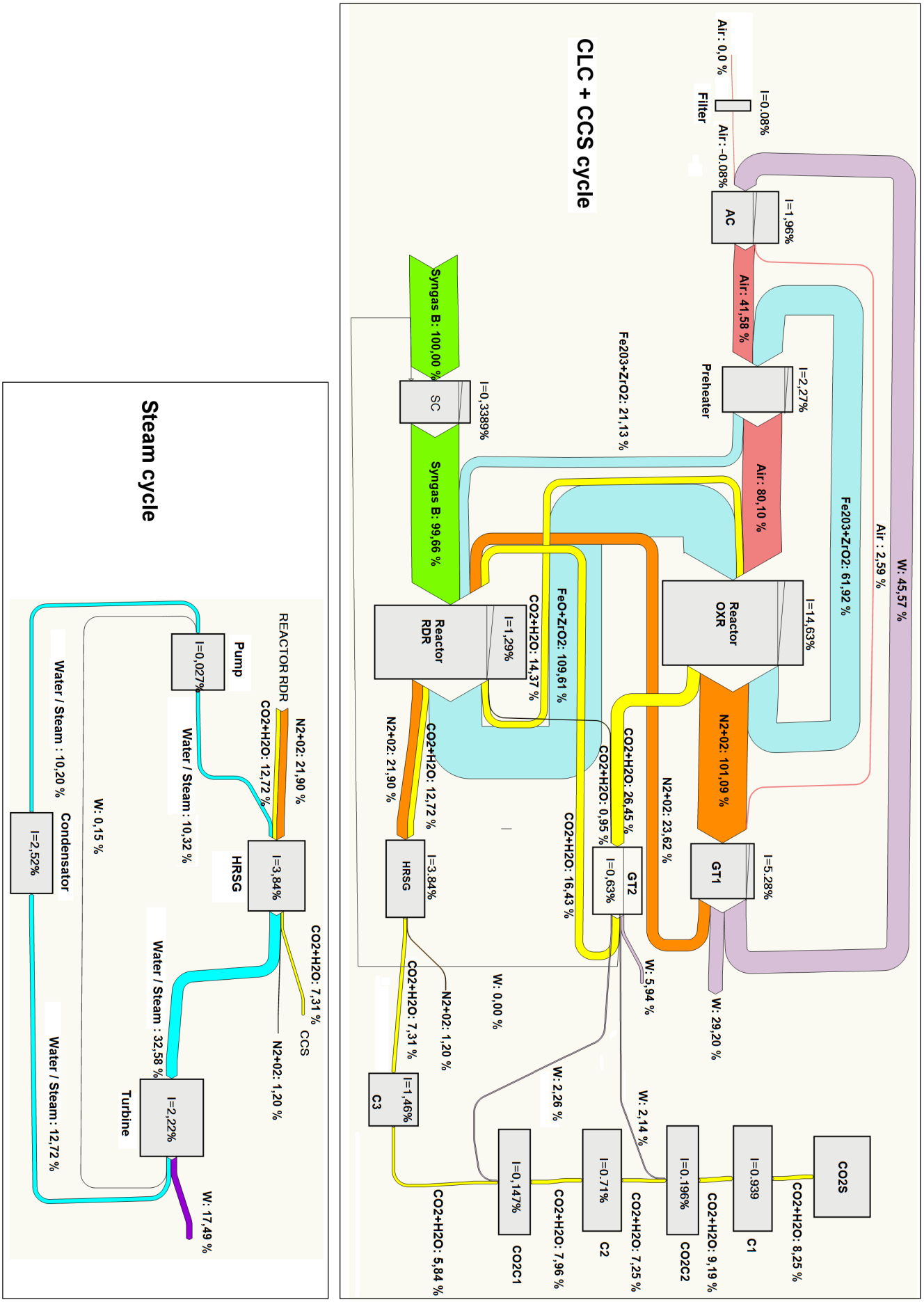

**Figure 16.** Grassmann diagram for syngas C. TIT = 1550 K, $p_r$ = 27 bar, $T_{red}$ = 814 K.

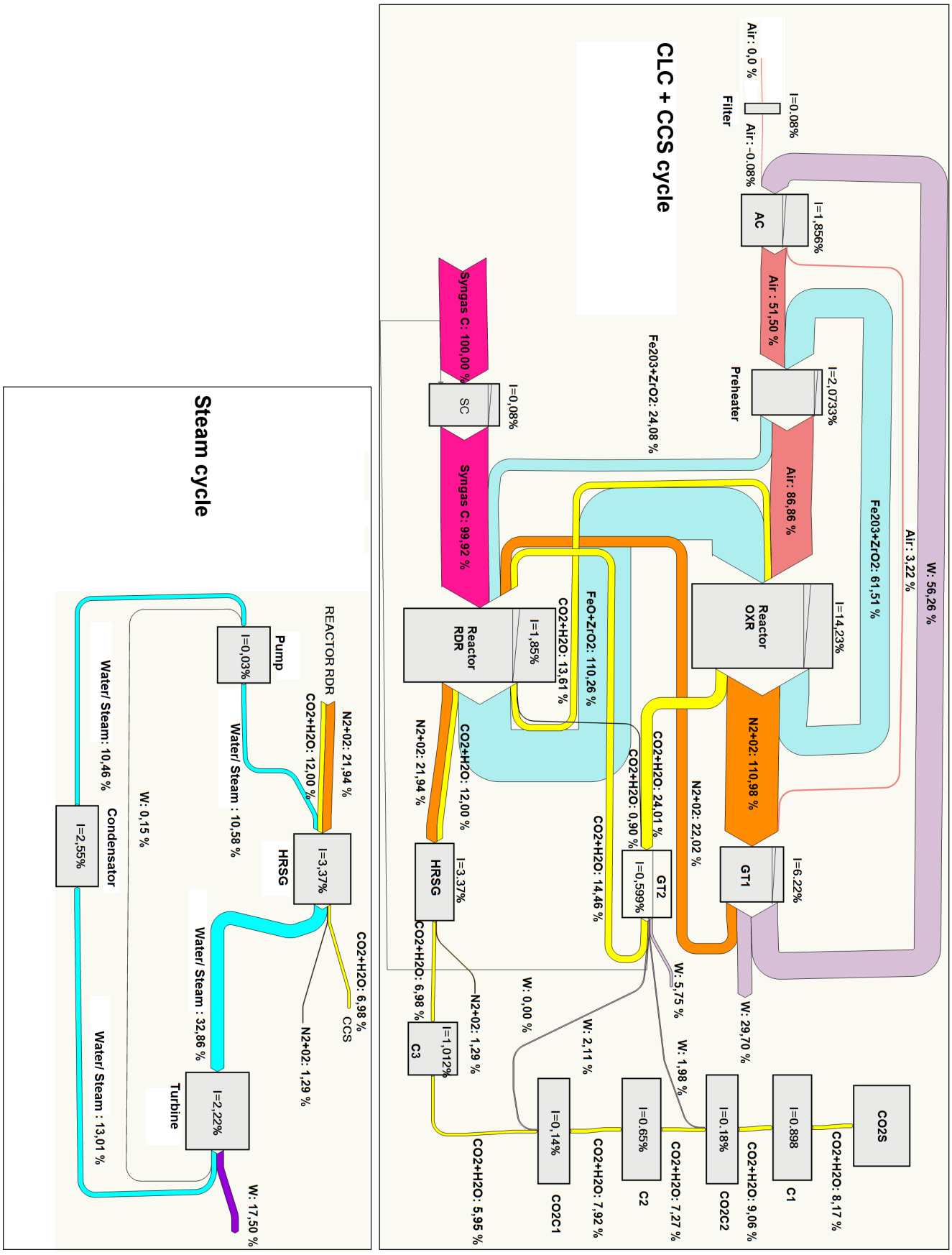

**Table 4.** Comparison between exergy flows of CLC and conventional gas turbine systems. TIT = 1550 K, $p_r$ = 20 bar.

| Fuel | Combustion type | $\dot{E}_{HRSG}$ (%) | $\dot{W}_{GT}$ (%) | $\dot{I}_{t_{comb}}$ (%) | $\dot{I}_{t_{rest}}$ (%) | $\dot{I}_{t_{all}}$ (%) |
|---|---|---|---|---|---|---|
| Syngas A | CLC | 35.15 | 39.26 | 15.97 | 9.62 | 25.59 |
| | conventional | 33.60 | 38.60 | 20.92 | 6.88 | 27.80 |
| Syngas B | CLC | 34.62 | 39.53 | 15.92 | 9.93 | 25.85 |
| | conventional | 33.24 | 38.73 | 20.97 | 7.06 | 28.03 |
| Syngas C | CLC | 34.84 | 38.89 | 16.25 | 10.02 | 26.27 |
| | conventional | 33.09 | 38.80 | 20.98 | 7.13 | 28.11 |

savings. On the other hand the additional heat an pressure losses and the exergy destruction in heat exchangers involved in the CLC case, makes the total exergy losses more similar when the whole gas turbine system is considered. Still, the overall exergy loss is lower and the power generated is slightly higher for the CLC cycle. In addition, more exergy is carried by the stream entering the HRSG, expecting a little more of power to be obtained by the steam cycle. This point can be surprising at first sight, since some heat must be taken from the gas streams outgoing the turbines in the case of the CLC system. Nevertheless, it must be kept in mind that the expansion in GT2 is carried out down to a pressure of 1.5bar (for optimization purposes when $CO_2$ compression takes part, see section 3.2) instead to approximately the atmospheric pressure, as it happens in a conventional gas turbine. Thus, the temperature of this stream is increased in relation with the conventional gas turbine. Even so, the power produced by the ensemble is a little bit larger for the CLC gas turbines system.

## 4. Conclusions

This work presents an exergy analysis of a combined cycle with carbon sequestration and storage in base of a CLC combustion system. Syngas is used as fuel looking to investigate a possible integration with a previous gasification process. Three syngas compositions have been studied in order to determine the influence of hydrogen and carbon monoxide content on results. The exergy input and output flows, power production and consumption and exergy losses have been quantified for the whole power plant as well as for every component individually. A range of operating conditions have been simulated and an optimization of the main thermodynamic parameters of the CLC cycle has been carried out. In addition, the exergy performances of gas turbine systems with conventional and CLC combustion systems have been compared with the object of giving some insight into the CLC concept from an exergetic point of view.

The following points summarize the main conclusions of the study:

- The exergy destruction in the combustion chemical transformation with CLC is about three quarters that of the conventional combustion. Even considering the additional exergy losses that happen in the CLC case, the power produced by the gas turbine system is somewhat higher for the CLC system.

- The exergy efficiency of a CLC gas turbine combined cycle including a carbon sequestration and storage module is very notable. Figures of about 50% are reached including the important power consumption for $CO_2$ compression up to the storage pressure.
- The optimal pressure ratios from an exergetic point of view is moderate and easily attainable for modern gas turbine systems, although some differences between fuels have been found. Furthermore, a wide range of pressure ratio still gives a good performance due to the peculiar behavior of the efficiency curves.
- Chemical equilibrium calculations confirm that the heat balance can be achieved at the reduction reactor with a high degree of fuel oxidation ratio in a temperature range of 720–820 K.
- The combination of some thermodynamic effects induces a peculiar tendency change of the optimal reduction temperature with the operating conditions when the so-called *reduction reactor heating uncoupling point* is reached. This phenomenon implies an extra power production in the CLC based gas turbines in comparison with the expected tendency.
- The fuel's composition has an important role in relation to the exergy flows that take place in the CLC cycle. The influence of fuel composition is much more important in determining the optimal cycle conditions than in case of conventional combustion, due to the complex dynamics regarding chemical equilibrium and heat flows and balances in CLC reactors.

Although at this moment we can say that we are far from the technological maturity required for an industrial use, the results point out that CLC is a promising technique with a great potential for power generation with high efficiency and $CO_2$ emissions almost nil.

## Conflicts of Interest

The authors declare no conflict of interest.

## References

1. Chiesa, P.; Consonni, S. Natural gas fired combined cycles with low $CO_2$ emissions. *J Eng Gas Turb Power* **2000**, *122*, 429–436.
2. Urech, J.; Tock, L.; Harkin, T.; Hoadley, A.; Maréchal, F. An assessment of different solvent-based capture technologies within an IGCC-CCS power plant. *Energy* **2014**, *64*, 268–276.
3. Hagi, H.; Bouallou, Y.L.M.M.N.C. Performance assessment of first generation oxy-coal power plants through an exergy-based process integration methodology. *Energy* **2014**, *69*, 272–284.
4. Ishida, M.; Jin, H. A new advanced power-generation system using chemical-looping combustion. *Energy* **1994**, *19*, 415–422.
5. Zhang, X.; Han, W.; Hong, H.; Jin, H. A chemical intercooling gas turbine cycle with chemical-looping combustion. *Energy* **2009**, *34*, 2131–2136.
6. Anheden, M.; Svedberg, G. Exergy analysis of chemical-looping combustion systems. *Energy Conv Manag* **1998**, *39*, 1967–1980.

7. Anheden, M. Analysis of gas turbine systems for sustainable energy conversion. PhD thesis, Royal Institute of Technology, ISRN KTH/KET/–11–SE, Stockholm, Sweden, 2000.
8. Jiménez, Á.; López, I.; González, C.; Nieto, R.; Rodríguez, J. Energetic analysis of a syngas-fueled chemical-looping combustion combined cycle with integration of carbon dioxide sequestration. *Energy* **2014**, *76*, 694–703.
9. Jing, D.Z.X. Chemical amplifier and energy utilization principles of heat conversion cycle systems. *Energy* **2013**, *63*, 180–188.
10. Ishida, M.; Jin, H. A novel chemical-looping combustor without $NO_x$ formation. *J Ind Eng Chem* **1996**, *35*, 2469–2472.
11. Consonni, S.; Lozza, G.; Pelliccia, G.; Rossini, S.; Saviano, F. Chemical-looping combustion for combined cycles with $CO_2$ capture. *J Eng Gas Turb Power* **2006**, *128*, 525–534.
12. Nieto, R.; González, C.; López, I.; Jiménez, Á. Efficiency of a standard gas-turbine power generation cycle running on different fuels. *Int J Exergy* **2011**, *9*, 112–126.
13. Mínguez, M.; Jiménez, Á.; Rodríguez, J.; González, C.; López, I.; Nieto, R. Analysis of energetic and exergetic efficiency, and environmental benefits of biomass integrated gasification combined cycle technology. *Waste Manage Res* **2013**, *31*, 401–412.
14. Kotas, T.J. *The exergy method of thermal plant analysis*; Butterworths: London, UK, 1985.
15. Escudero, M.; Jiménez, Á.; González, C.; Nieto, R.; López, I. Analysis of the behavior of biofuel-fired gas turbine power plants. *Therm Sci* **2012**, *16*, 849–864.
16. http://webbook.nist.gov/chemistry/form-ser.html. online (last access on 30/07/2014), National Institute of Standards and Technology, U.S. Department of Commerce.
17. Daubert, T.E.; Danner, R.P. *Physical and thermodynamic properties of pure chemicals: Data compilation*; Hemisphere Publishing Corporation: New York, NY, USA, 1989.